JOURNAL OF GEOPHYSICAL RESEARCH, VOL. 87, NO. B2, PAGES 979-989, FEBRUARY 10, 1982

Displacement of Surface Monuments: Horizontal Motion

FRANK WYATT

Institute of Geophysics and Planetary Physics, Scripps Institution of Oceanography, University of California at San Diego, La Jolla, California 92093

Measurements of tectonic deformation depend on both accurate instrumentation and adequate coupling of the apparatus to the earth's crust. Existing techniques, capable of resolving the signals of interest (strain rates of 10 nϵ/yr), are mainly observatory based. The limitation in the baselength of these instruments (~1 km) results in a requirement that the reference monuments be exceptionally stable (10 μm/yr). However, records from Piñon Flat Observatory, California, show that the actual horizontal displacements for massive near surface monuments, emplaced in competent, weathered granite, are of the order of 50 μm/yr. The low noise level of the strain measurements at this site indicates that this magnitude of monument displacement is abnormally small. Until high-accuracy geodetic techniques are developed, sophisticated monuments (or monument monitoring devices) will be necessary to record faithfully continuous crustal deformation.

1. INTRODUCTION

Most techniques currently used to monitor continuously the deformation of the earth's crust employ instruments which measure over a limited baselength, almost always less than 1 km. Associated with this limitation is a requirement that the reference monuments, used as the fiducial points in the measurements, be well coupled to the crustal rocks. Because crustal deformations are both small in magnitude and occur very slowly, monument instabilities are likely to be the limiting factor in many crustal dynamics studies.

Even in areas of current tectonic activity the expected deformational signals may be so small as to be masked by undesirable monument displacements. That this is the situation is indicated by the measurements made at Piñon Flat Observatory (PFO), located in southern California. A collection of instruments has been operated at PFO since 1971 (see *Wyatt and Berger* [1980], for a list), with particular emphasis on the measurement of crustal strain using three 731-m laser strainmeters described by *Berger and Lovberg* [1970]. Although the observatory is situated only 12 km from the active San Jacinto fault zone [*Thatcher et al.*, 1975; *Sharp*, 1967], the dominant low-frequency signals recorded at the site are caused by environmental changes affecting the near-surface materials.

In an attempt to understand and compensate for the nontectonic (low frequency) displacements, three experiments were conducted at PFO. (1) Tiltmeters were fabricated to mount directly on the sides of the long (3 m) granite columns used as reference monuments for the strainmeters. These sensors served to detect the tilt of the granite columns and thereby to establish the horizontal motions at the tops of the columns relative to their bottoms. (2) An array of shallow borehole tiltmeters was deployed [*Wyatt and Berger*, 1980] in an effort both to understand the limitations of the particular instrumentation and to determine the spatial coherence of the near-surface displacements. (3) An instrument was designed and constructed to measure the horizontal motion of a surface monument relative to the material below. This device, called an 'optical anchor,' has been in operation for more than 1 year.

Paper number 1B1461.
0148-0227/82/001B-1461$01.00

Naturally, the implications of these investigations are limited in scope by the nature of the materials and the processes which affect the surface layers at PFO. However, the observatory is located on ground that is unusually well suited for monitoring crustal deformations. Evidence for this is provided by the records of the three strainmeters at the site. These observations show unsurpassed low strain noise [*Berger and Levine*, 1974], linear response to tidal strains [*Agnew*, 1981], and agreement with an elastic model of deformation due to earthquakes [*Wyatt*, 1980]. It is likely that the monument displacements recorded at PFO are representative of the lower range of motion for markers used in geophysical studies. If this is true, then current observatory-based instrumentation will require additional improvements in order to record crustal strains.

2. GEOLOGICAL SETTING

In selecting a site for monitoring tectonic deformation, proximity to a region of active faulting is most important. It is also desirable to choose a location that is situated on competent material. If long baselength instrumentation (1 km) is to be installed, the terrain must be sufficiently smooth. Unfortunately, in tectonically active areas the nonsedimentary surfaces are usually rugged. Gentle topography is more often associated with mature surfaces that have weathered to a stable base level without disturbance by recent crustal motions.

Pinyon Flat, which is located in southern California some 12 km northeast of the San Jacinto fault system and 25 km southwest of the San Andreas fault zone (33.609°N, 116.455°W), is an area that has the desired properties. The flat is situated on the northernmost flank of the Santa Rosa Mountains in the Peninsular Range Province. Roughly 12 km^2 in area, the flat is bounded by Asbestos Mountain to the north, Deep Canyon to the east, Santa Rosa Mountain to the south, and Palm Canyon to the west. Figure 1 shows a generalized map of the pertinent geological features and a sectional profile of the area, indicating the smooth topography of the flat between 'PFO' and 'Edge.'

There are several possible explanations as to why such an isolated flat surface is found at these elevations (1300

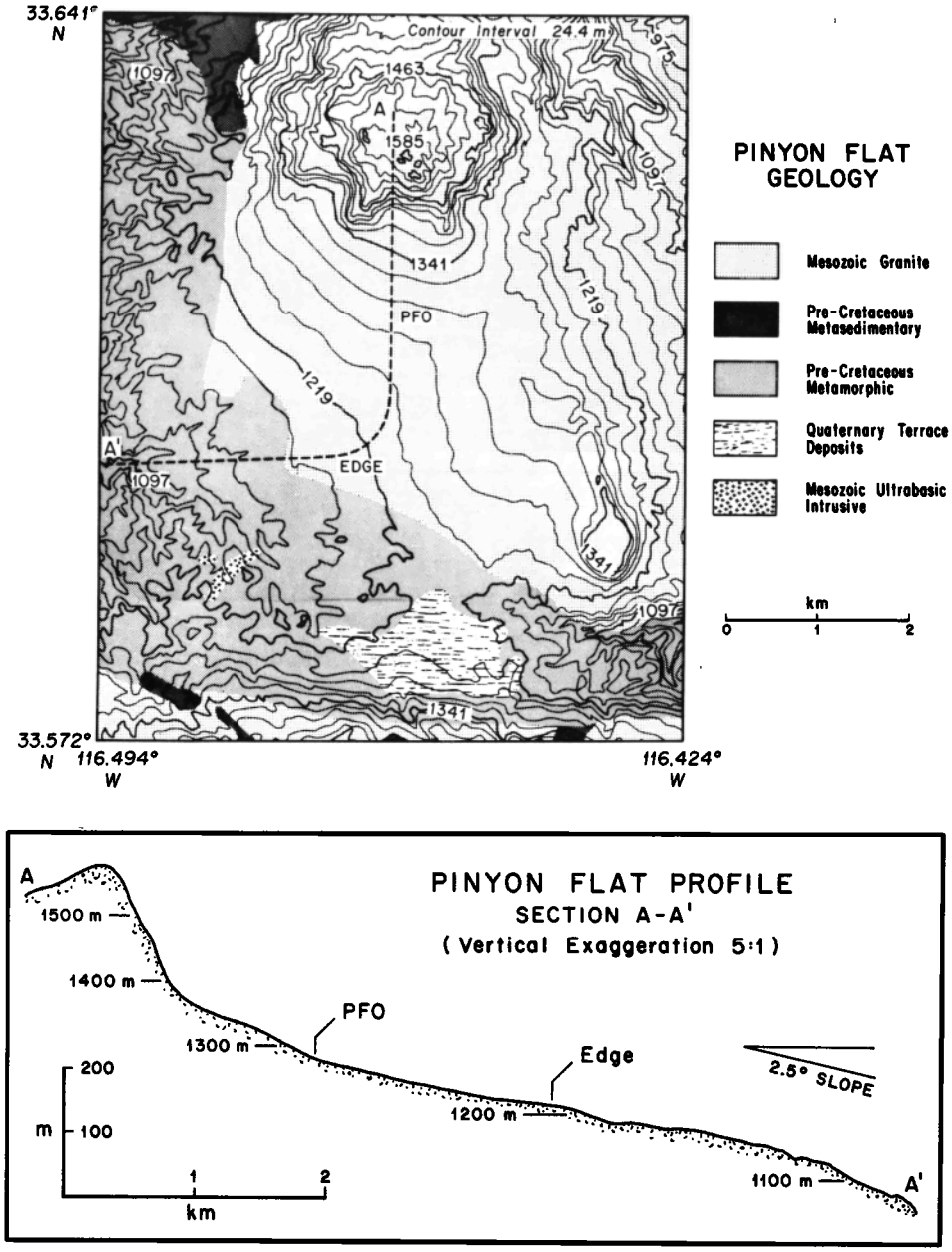

Fig. 1. Generalized map of the geologic features at Pinyon Flat, California [*Rogers*, 1965], and a sectional profile from Asbestos Mountain (A) to Palm Canyon (A'). The location of Piñon Flat Observatory is labeled PFO.

m). Undoubtedly, part of the reason is the nature of the crystalline rocks which underlie the area. The rocks are composed of Pinyon Flat granodiorite [*Foster*, 1976] of middle Cretaceous age (90—100 m.y. B.P.). This rock is unusually rich in biotite, which causes rapid weathering because of its expansion when exposed to moisture [*Isherwood and Street*, 1976]. Weathering causes the near-surface rock to decompose (via granular disintegration) to grus.

Jahns [1954] suggested three possible mechanisms for the development of low-relief surfaces on pre-Cenozoic terrain of crystalline rocks in the Peninsular Range Province. (1) The areas may be remnants of a single extensive peneplain, called the Southern California peneplain, that have been differentially uplifted by Quaternary faulting. (2) Some of the surfaces may be exhumed features that were originally formed in pre-Quaternary time and only recently reexposed. Some support for this mechanism is available near Pinyon Flat (see lower portion of map in Figure 1) where Quaternary terrace deposits are isolated on older rocks. (3) Finally, the surfaces may have formed locally by erosion to a new base level. Such a surface of low relief on exposed bedrock, when formed in a semiarid region and situated between an alluvial valley and a mountain, is commonly called a pediment (see, for example, *Cooke and Warren* [1973]). The concave form of the topography (toward the SW), the thin veneer of weathered material, and the size of the area are all features in common with pediments. Absent from the Pinyon Flat area is a base level defined by an alluvial plain.

This unusual situation may be explained by considering a mechanism presented by *Wahrhaftig* [1965]. Wahrhaftig observed that exposed granites weather much more slowly

than those rocks which are buried and hence are moist for longer periods of time. Perhaps the relatively unweathered outcrops exposed on the southwest edge of the flat tend to act as a local base level. Another possibility is that the change in lithology near the edge of the flat is responsible for reducing the erosion in that area.

Whatever the cause or combination of causes responsible for the creation of the surface, the most significant process currently affecting the surface layers is weathering. The near surface (at a depth of 0.5 m) is subject to a yearly temperature range of 18°C, with daily variations of the order of 0.3°C. On rare occasions, ground frost will reach a few centimeters in depth. The average annual rainfall has been 25.4 cm for the period 1971–1980. Normally, this precipitation occurs in the form of infrequent (but intense) thundershowers in the months of August and September, along with less substantial prolonged winter storms. The top 1 m of ground at the site is nearly fully decomposed granodiorite. Below this level the weathered rock grades to highly competent grus at a depth of roughly 3 m. This material has decomposed in situ; dikes and other features of the rock are readily identifiable. At this depth, standard soil-moving machinery is no longer effective in excavating material. However, once a section of rock is removed, it is found to be friable. The majority of the reference monuments at PFO were emplaced in the material at this depth. Conventional benchmark rods reach the depth of refusal in this layer (1–3 m). Evidence provided by drilling suggests that below 3 m to a depth of 25 m the material grades from grus to grus with corestones and finally to jointed granodiorite as illustrated in the right half of Figure 2.

A shallow seismic refraction survey supports these observations. Figure 2 presents the possible range of the compressional seismic velocities for two locations at Pinyon Flat. These velocity corridors were determined by J. Orcutt (personal communication, 1980), using a procedure described by *Garmany et al.* [1979]. The heavy solid lines are the extremal bounds on the solution to the seismic travel time inverse problem at PFO, based on the limited and inexact nature of the field observations. The dashed lines are the bounds at Edge. All possible models of the velocity profile lie within these bounds. The light solid lines indicate particular models that may be used to generate the observed travel times. It is unlikely that the layering shown in these models exists; rather, the velocities probably increase smoothly with depth as the effects of weathering diminish.

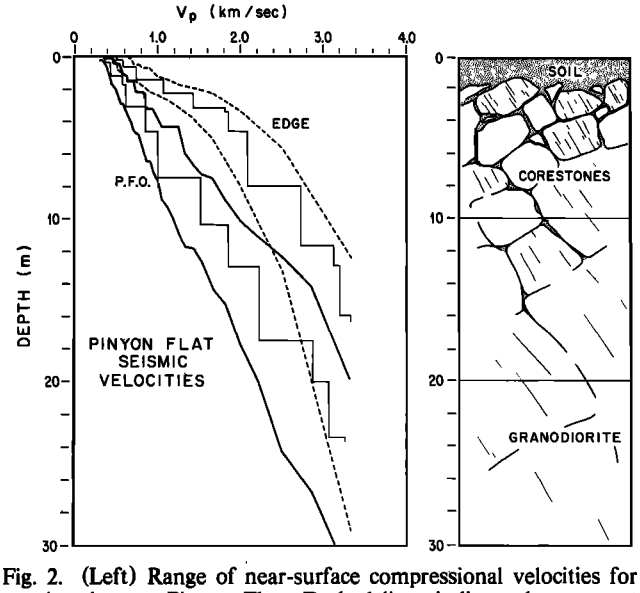

Fig. 2. (Left) Range of near-surface compressional velocities for two locations at Pinyon Flat. Dashed lines indicate the range at Edge (see Figure 1), and the solid lines indicate the range at PFO. (Right) An illustration of the structure as suggested by borehole drilling observations.

There is a marked difference between the seismic velocities at PFO and Edge. Velocities less than 2 km/s, normally associated with sediments, are limited to depths of 8 m at Edge but may extend as deep as 18 m at PFO. The PFO profile is representative of most of the area, while the Edge data are more characteristic of the material at the limits of the flat, where outcrops (tors) are prevalent. Evidently, the weathering is less near the edge of the flat, supporting Wahrhaftig's hypothesis for the formation of such surfaces.

Below 20 m the velocities at both locations tend to values that are characteristic of granodiorite subjected to low confining pressures (0.5 MPa) [*Birch*, 1960]. Analysis of a core sample from PFO established the seismic velocity at a depth of 38 m to be 4.8 km/s (C. Sondergeld, personal communication, 1980). This value is in excellent agreement with the mean velocity obtained by extrapolating the linear trend of the extremal bounds in Figure 2 and is representative of crustal rock velocities. We may assume that instruments not adequately coupled to the rock below the material with low velocities (~20 m at PFO) will be sensitive to the displacements inherent in the weathering process.

3. Instrument Description

a. Pier Tiltmeters

The need for stable tiltmeters to monitor the tilt of granite monuments at PFO was first recognized in 1973. At that time, two of the three 731-m laser strainmeters that now occupy the site were in operation. These strainmeters continuously monitor the change in distance between the top of columns (1 m^2 in cross section) that are composed of black granite (technically, San Marcos gabbro), commonly used for optical tables. It was observed that major changes in the recorded strain rates at the observatory correlated with local precipitation, particularly when it exceeded 3 cm. The magnitude of the strain change and its coincidence with periods of substantial precipitation indicated that the granite columns were not well coupled to the underlying bedrock. Preliminary investigations established that the columns were undergoing large tilts in response to increased soil moisture. This was true in spite of the (apparently) competent nature of the material surrounding the base of the monuments.

The six strainmeter monuments were emplaced and supported in different manners. Four of the columns (North, South, East, and West) were set freestanding in excavated holes partially filled with nonshrink grout, with additional grout added to a height of 1 m above the bottom of the holes. The remaining two monuments

TABLE 1. Strainmeter Monuments

Monument	Length, m	Depth, m	Slope of Surface	Displacement Rate, μm/yr	Annual Cycle Amplitude, μm	Annual Cycle Phase	Standard Deviation, μm
North	3.8	2.7	5°S	32 N	8.5	145°	26
South	2.9	1.8	2°S	47 N	74.	81°	70
West	4.6	3.2	1°W	26 E	3.8	136°	21
East	4.6	2.7	0°	140 E	52.	−131°	92
Northwest	1.2	3.4	5°SE				
Southeast	1.7	3.3	3°NW				

Slope of surface refers to the component along the axis of measurement. Stated direction is down-slope. Phase of annual cycle is given relative to start of year for cosine wave (minus indicates lag). Standard deviation is from linear trend after removing annual cycle.

(Northwest and Southeast) were simply cemented to the floor of underground vaults. Table 1 presents the pertinent dimensions of these monuments.

Small tiltmeters were designed to mount directly on the sides of the granite columns. The transducers were fabricated of fused silica with a mass suspended on fine wires. Motion of the mass was sensed using a differential capacitance detector. A small plastic enclosure was placed around the device to provide limited temperature control and reduce environmental effects from airflow and humidity changes. The overall stability of tiltmeters and electronics exceeded the design criterion of 1 μrad/yr (corresponding to a strain rate of 0.005 με/yr for a 731-m strainmeter and a column 3.7 m in length).

The signal from each of the six tiltmeters was multiplied by the appropriate pier length to compute the displacement at the top of the column relative to the bottom (see left half of Figure 3). The power spectral levels of the resultant strain data are among the lowest noise observations reported [*Berger and Levine*, 1974], and yet the strain records, even after being corrected for pier tilt, were still correlated with the pier tiltmeter records. This suggests that the columns were not simply tilting about their bases. Estimates of the magnitude of the horizontal displacements at the base of the columns are presented in section 4*a*.

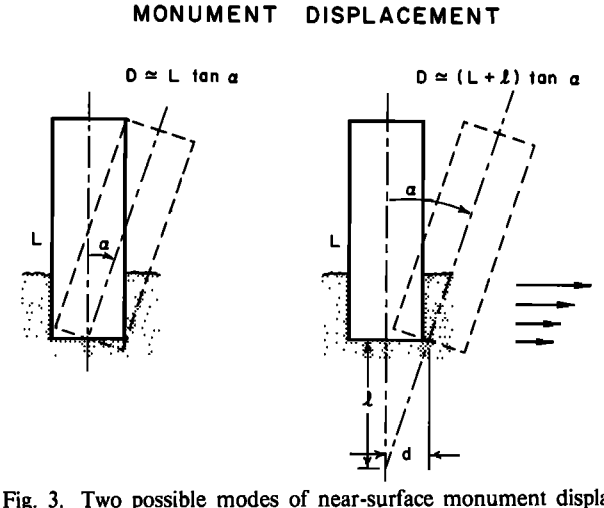

Fig. 3. Two possible modes of near-surface monument displacement. The diagram on the right shows the inferred motion of the monuments at Pinyon Flat as deduced from the pier tilt and strain observations.

b. Shallow Borehole Tiltmeters

An array of four shallow borehole biaxial tiltmeters (Kinemetrics, Inc., San Gabriel, California, model TM-1B) was deployed at the observatory in early 1977. Data from the array were to be used to investigate both the inherent limitations of the tilt transducer and the spatial coherence of the near-surface tilt field. It was established that the dominant signals evident in the records were not coherent [*Wyatt and Berger*, 1980]. The magnitude of the signals, which were representative of those recorded at other locations, exceeded the noise levels determined for the tiltmeter transducer alone [*Johnston*, 1976]. The most likely source of the observed signals was found to be the local rock surrounding the instrumentation.

The tiltmeters were emplaced in a manner described by *Morrissey* [1977]. Large access holes, 1 m in diameter,

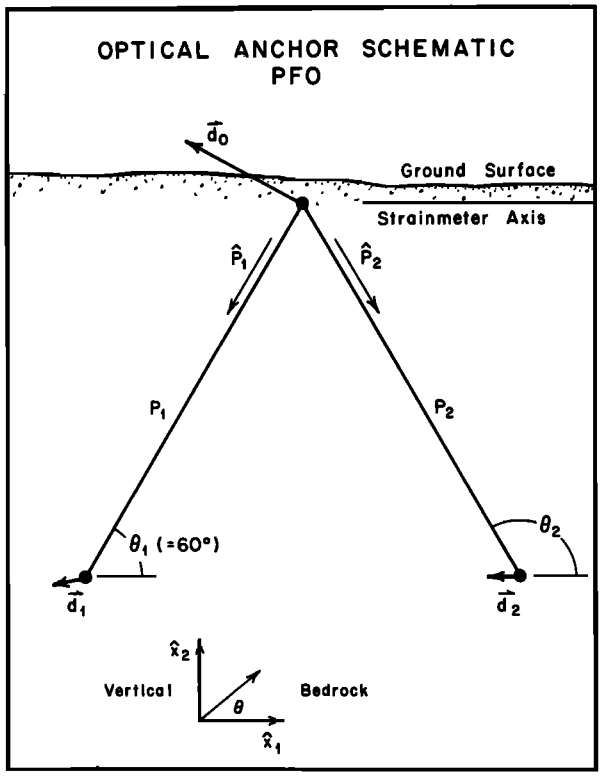

Fig. 4. Schematic of the optical anchor. The anchoring points for the instrument at PFO are located at a depth of 24 m.

were drilled to a depth 3.5 m and cased with thin-walled corrugated steel tubing. A 12-cm-diameter hole was drilled from the bottom of the large hole to a total depth of 5 m. The meter-long tilt transducer was placed in the smaller hole, while fine-graded silica sand was packed around the unit. The mean depth of tiltmeters was 4.5 m.

c. Optical Anchor

The inadequacy of the data from the pier tiltmeters, to remove completely from the strainmeter records the energy correlated with intense rainfall, led to a search for a more direct method of measuring monument displacements. The instrument developed for this purpose is termed an 'optical anchor' [*Wyatt et al.*, 1982]. The device is simply a long baselength shear strainmeter, capable of measuring the horizontal component of shear in the top layers of the crust.

The principles of the optical anchor are outlined in Figure 4. A laser interferometer measures the difference in length of the two paths P_1 and P_2. At some depth well below the instrumentation a coordinate system may be defined in the (stable) bedrock, with the x_1 axis aligned in the direction of the horizontal displacement measurement. We assume that the two anchoring points are well coupled; that is, either $\mathbf{d}_1 = \mathbf{d}_2$ or $|\mathbf{d}_1|, |\mathbf{d}_2| \ll |\mathbf{d}_0|$. This assumption is essential and is justified by the observations to this date [*Wyatt et al.*, 1982]. If this assumption is true, then the output of the optical anchor is given by $D = \mathbf{d} \cdot \hat{x}_1$, where $\mathbf{d} \equiv \mathbf{d}_0 - \mathbf{d}_1 \cong \mathbf{d}_0 - \mathbf{d}_2$. This is simply the horizontal displacement of the surface monument relative to the material at depth.

The implementation of this concept required an unusual amount of engineering. Two boreholes inclined at 30° to the vertical were drilled some 26 m from a point roughly 2.5 m below the surface. The holes were located in the vertical plane aligned with the azimuth of the Northwest-Southeast strainmeter and intersected at a point slightly above the Northwest strainmeter end pier. Optical retroreflectors were mounted near the bottoms of these holes, and an inexpensive alignment laser was utilized in an equal-arm Michelson interferometer to determine the displacement.

4. DISCUSSION OF OBSERVATIONS

The discussion of monument displacements presented in this section is divided according to the type of instrumentation. The observations from each instrument are then further classified according to the frequency content of the dominant signals. The highest-frequency signals of interest are those associated with seismic events. The accelerations from nearby earthquakes are often a significant fraction of gravity and induce abrupt monument displacements. At lower frequencies, diurnal motions are recognizable; they are primarily caused by thermoelastic effects near the surface. At frequencies near 1 cycle per year, the driving forces responsible for the displacements are harder to isolate. Not only must annual thermoelastic effects be considered as a factor, but seasonal weather patterns systematically alter the conditions in the surface layers. The final family of signals to be discussed are those that are episodic in nature (e.g., those related to unusual precipitation) and the long-term linear trend of the observations. These have been grouped together owing to the length of the data sets. Without a long data base it is often not possible to establish the trend independently of the episodic events.

a. Pier Tiltmeters

The records of the laser strainmeters at PFO provide us with evidence that the end piers are not stable. The underlying assumption used to reach this conclusion is that the true regional strain rates are not expected to be correlated with sudden changes in the local environmental conditions. However, after the strain observations are corrected for the displacements of the end piers due to tilts, the major changes in the strain rates remain associated with the periods of heavy precipitation. Further, the corrected strain records are still correlated with the pier tilt observations. This can be seen by comparing the traces labeled 'Corrected Strain,' 'East Monument Correction,' and 'West Monument Correction' in Figure 5.

For two of the strain records (North-South and East-West) it is possible to reduce the variance of the corrected strain observation by a factor of 4 by least squares fitting (LSF) the corresponding pier tilt records to the uncorrected strain. The resulting signal for the East-West strainmeter is presented in Figure 5. The scaling factors established by the LSF process are systematically greater (1.3 ± 0.15) than the proper coefficients used to calculate the displacements at the top of the column due to tilt. This is the case for the four columns that are embedded in the surface material. A simple model for such displacements is illustrated in the right half of Figure 3. If a pier of length L were to rotate through an angle α about a point l beneath its base, rather than at the base (as supposed before), then the top of the column would be subject to a displacement of $(L + l) \tan \alpha$. While a tiltmeter can faithfully measure the tilt α, it cannot accurately monitor the total displacement under these circumstances.

The situation is different for the two short columns (NW and SE) at PFO. Although the uncorrected strain records and the pier tilt records display similarities, there is no fixed relationship that may be used to reduce the variance of the strain observations. There is little doubt that the larger variations in all three strain records are the result of unstable end piers.

Both of these observations may be explained in terms of near-surface horizontal shearing. Let x be a horizontal direction and U_x the associated displacement. Similarly allow z to be directed vertically and U_z to be the vertical displacement. Then either $\partial U_z/\partial x$ (tilt of a horizontal element) or $\partial U_x/\partial z$ (tilt of a vertical element, which we shall call shear) will cause a tilt of the embedded end piers and hence an apparent strain. Since the NW and SE piers were simply set on the floor of underground vaults, they may displace horizontally in response to shear but not necessarily tilt. The tilts of the longer columns may be considered the result of differential horizontal motion (shear). Quite simply, the LSF parameters indicate that the deeper materials are displacing less in response to the environmental factors than are the materials nearer the surface.

On the basis of the assumption that the true strain rates

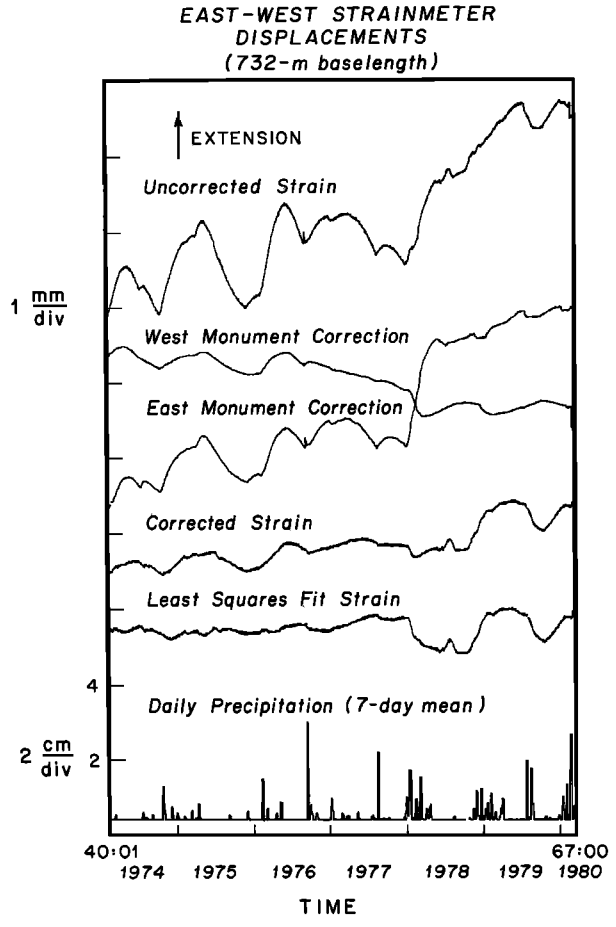

Fig. 5. Records from the 731-m East-West strainmeter at PFO, including the West and East monument tilt observations (converted into equivalent displacements) and the strainmeter displacements corrected in two different manners. Also presented is a record of the daily precipitation.

at PFO should be uncorrelated with the pier tilt corrections, the apparent horizontal displacements for the individual piers were calculated. Figure 6 presents the inferred pier displacement records. These series were derived by estimating the total tilt-related displacement for each column with the LSF process (fitting to the strain) and subtracting the true pier tilt displacement component. Although the fitting coefficients for subsets of the series vary slightly, they are generally stable to within 30%. This is remarkable in light of the variability of the environmental factors at PFO.

A notable change in this pattern is evident in the strain records in Figure 5, beginning in 1978. At this time the LSF strain record fluctuates more than the corresponding corrected strain. This indicates that the effective point of rotation of the East column moved closer to the base of the monument. In contrast to this the rainfalls of 1979 may have caused the opposite effect. The tilt signals display very little response to the substantial precipitation, but the strains are large. If the point of rotation were well below the column (or if this were a real strain), it would produce this result.

Examination of Figure 6 reveals that the largest displacement signals are correlated with the rainfall. Attempts were made to establish the filter weights that would produce the pier displacement records given the precipitation records at PFO (see *Wood and King* [1977], for an example of this procedure). This process was very successful when applied to selected portions of the data but generally unsuccessful for complete series. Apparently, the response of monuments to rain is not predictable using techniques such as least squares filtering, whereas the strain error signals may be estimated relatively accurately using the pier tilt records.

Table 1 lists the linear trends and standard deviations for the inferred pier displacements. The rates of displacement range from 26 to 140 μm/yr, with 50 μm representing the standard deviation from a linear trend after removing the annual cycle. There is no obvious relationship between the direction of the displacements and the local topography. Rather, the motions seem to be the result of repeated surface adjustments in response to changes in the soil conditions.

Very little can be determined about those signals with periods shorter than 1 day. Insufficient energy is present in the tilt series at high frequencies to establish a reliable estimate of the relationship of the tilt signals to the perturbations in the strain records. *Agnew* [1979] has reported that the observed pier tilt signals at a frequency of 1 cycle per day can be explained by tilt due to thermoelastic effects.

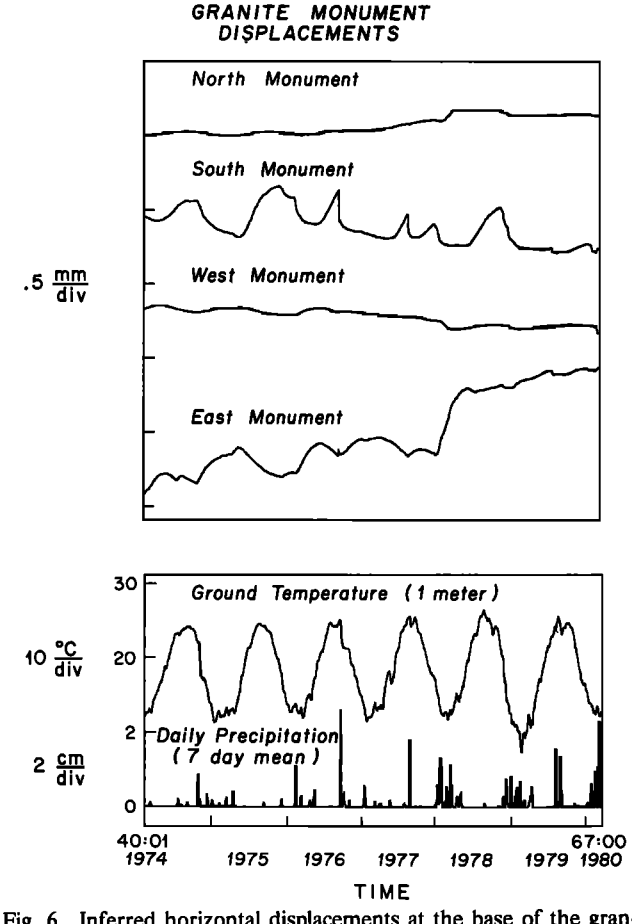

Fig. 6. Inferred horizontal displacements at the base of the granite monuments used in the laser strainmeter measurements (with coseismic offsets removed). In the lower panel the temperature at a depth of 1 m and the daily precipitation records are presented.

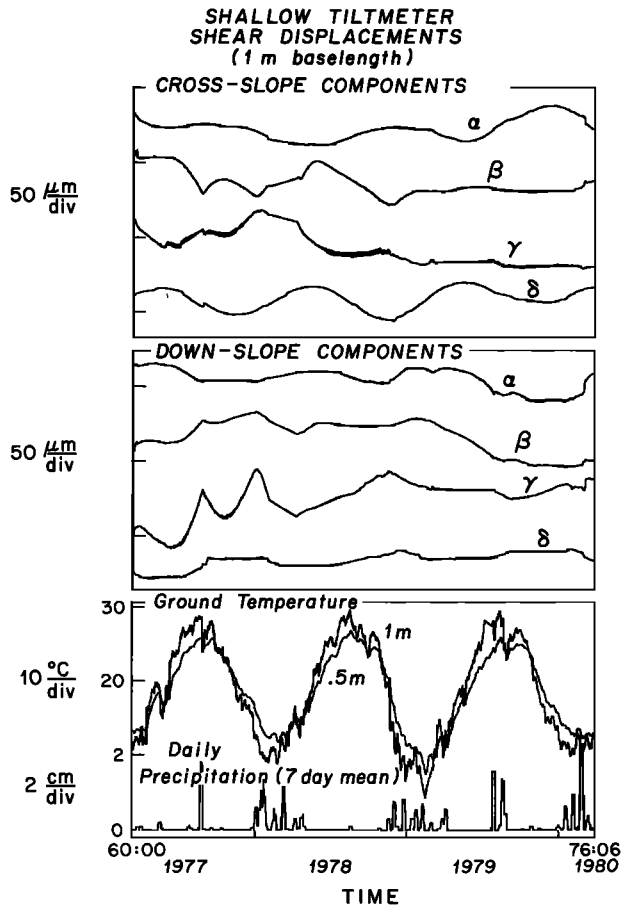

Fig. 7. Horizontal shear displacements at a depth of 4.5 m as recorded by the 1-m-long shallow borehole tiltmeters (with coseismic offsets removed). The upper panel displays the cross-slope components, the middle panel, the down-slope components, and the bottom panel, the ground temperature at 0.5 m and 1 m, along with the daily precipitation.

b. Shallow Borehole Tiltmeters

The shallow borehole tiltmeters at PFO may be used to obtain an independent estimate of near-surface horizontal displacements. The sensor packages are cylindrical, 5 cm in diameter, 107 cm in length, and installed with the long axis aligned vertically. Owing to their shape, the tiltmeters are primarily sensitive to shearing, $\partial U_x/\partial z$, rather than tilt, $\partial U_z/\partial x$. Of course, the magnitude of these two quantities should be identical at the traction free surface of a homogeneous elastic half space. However, the lack of agreement between adjacent horizontal tiltmeters at PFO suggests that a purely elastic model is not appropriate on this scale. A lower bound estimate of the local horizontal displacements at a depth of 4.5 m may be obtained by calculating the product of the length of the sensor (107 cm) and the observed tilt.

Two experiments were performed to establish the origin of the observed displacements. The material that was packed around the sensors, to couple them to the surrounding material, was considered as a potential source of noise. Strains of the order of 1 mε in the fine silica sand would be sufficient to produce the observed signals. During episodes of soil moisture changes, strains as large as this could be expected. However, subsequent to a major rainstorm an instrument was reinstalled in the same borehole, and the low-frequency signals (trends) were unchanged. A similar test was performed to establish that the cycle per day component of the tilt was not the result of temperature sensitive components in the sensor or the associated electronics. A transducer unit was rotated azimuthally through 180° and the cycle per day signal (referred to the ground) did not change. This established that the source of the signal was external to the tiltmeter instrumentation.

Figure 7 shows the tilt signals converted into displacement and rotated into components representing the down-slope and cross-slope components. A feature of the original records, which has been removed, is a very large excursion on three of the four tiltmeters occurring between days 23 and 93 of 1978. This interval was coincident with the first sustained precipitation at PFO since the installation of the tiltmeters. It is assumed that the displacements which took place at that time were the result of settling of the packing material surrounding the tilt sensors. These signals were not considered further and are not included in the estimates of displacements. However, the remaining signals are strongly influenced by the rainfall. Abrupt changes in the trends of the displacements are evident in most of the records. These events often last for months, with overall displacements as large as 30 μm.

The linear trend and annual cycle were calculated by fitting them to the observed records. Table 2 presents the results. Once again there is no clear relationship between the local topography and the linear drift component. The cross-slope components are approximately the same magnitude as the down-slope measurements, ranging from 2 to 10 μm/yr. Not surprisingly, these estimates of the horizontal displacement are much lower than those obtained using the pier tiltmeters and strainmeter records. This is due to the (improbable) assumption that the observed near-surface shearing only extends over the length of the instrument.

The phases of the annual cycle displacements are about the same as the phase of the temperature at a depth of 4.5 m. This result agrees with the computations of *Harrison and Herbst* [1977] for thermoelastic strains on a sloping surface. For an applied periodic temperature of the form $T(t) = T_0 \cos(2\pi ft)$, where f is the frequency and t is time, they determined that the horizontal shear should be

$$\frac{\partial U_x}{\partial z} = \tfrac{1}{2}\,\frac{1+\sigma}{1-\sigma}\,\beta T_0 e^{-k(z-z_0)} \sin(2\alpha)\cos\phi$$

$$\phi = 2\pi ft - k(z - z_0) \qquad (1)$$

In this equation U_x is the down-slope horizontal displacement, z is the measured depth (z_0 is the depth where $T(0) = T_0$), σ is Poisson's ratio, β is the coefficient of linear thermal expansion, α is the slope of the surface, and k is the thermal wave number ($k = 2\pi/\lambda = (\pi f/K)^{1/2}$, where K is the thermal diffusivity). Substituting representative values for the variables $\sigma = 0.33$, $\beta = 2 \times 10^{-5}$ °C^{-1}, $T_0 = 8.85$°C, $z_0 = 0.5$ m, $k = 0.45$ m^{-1}, $\alpha = 5°$, $z = 4.5$ m), we find the amplitude of the shear to be 5 μrad. While the magnitude and phase compare favorably with the observed values, the sign of the

TABLE 2. Near-Surface Tiltmeters

Component	Slope of Surface	Azimuth	Displacement Rate, μm/yr	Annual Cycle Amplitude, μm	Annual Cycle Phase	Standard Deviation, μm
Alpha DS	5.4°	185°	−4.1	5.1	−103°	3.7
Alpha CS	0	275°	1.8	4.8	51°	5.2
Beta DS	5.4°	185°	−7.9	3.1	20°	8.1
Beta CS	0	275°	−4.0	6.1	−133°	4.4
Gamma DS	4.5°	185°	7.7	6.3	36°	7.4
Gamma CS	0	275°	−10.4	4.5	−3°	5.5
Delta DS	4.1°	290°	3.8	3.5	50°	2.0
Delta CS	0	20°	2.6	8.9	−124°	1.6

DS indicates down-slope component. CS indicates cross-slope component. Phase of annual cycle is given relative to start of year for cosine wave (minus indicates lag). Standard deviation is from linear trend after removing annual cycle.

observed down-slope shear is not consistent with the theory. Further, the model predicts that the cross-slope components should be zero, which they are not. Even instruments located within 10 m of one another record a signal of opposing polarity. It is likely that the observed signals are indeed driven by thermoelastic strains but the near surface is not sufficiently uniform to be modeled as a tilted homogeneous half space.

Neither the phases nor the magnitudes of the observed diurnal displacements are consistent, suggesting that the signals are locally generated. The most striking feature of the cycle per day noise is its variability. In the course of prolonged droughts at the observatory, the amplitudes of the diurnal displacements increase. This change in amplitude has been as large as a factor of 5. At the onset of rain the diurnal signals generally reduce in amplitude. We know from theoretical calculations that at the (relatively) high frequency of 1 cycle per day the significant thermoelastic strains are limited to the very near surface (~0.5 m). How these surface tractions induce large strains at depth during periods of soil desiccation is unknown. Perhaps the properties of the surface material (thermal conductivity, rigidity, etc.) become increasingly inhomogeneous as the soil moisture escapes.

Seismic accelerations, resulting from earthquakes, are observed to cause the tiltmeters to displace. Generally, when the accelerations are less than 0.005 g, the sensors are not permanently disturbed. This is the situation for most teleseismic events. However, during the passage of seismic waves from local earthquakes (magnitudes 3—5 at distances of 15 km), horizontal accelerations at the site are often as much as 0.1 g. The resulting static offsets of the tiltmeters range from 0.02 to 4 μm. Because of the rapid onset of these inconsistent steps it is not possible to establish whether the displacements are representative of the surface layer or merely an adjustment of the transducer packing material.

c. Optical Anchor

The optical anchor records the horizontal displacement of a surface (z_0) monument relative to two points at depth ($z_1 = z_2$). Mathematically, the measurement may be represented as $\Delta U_x/\Delta z$, where the partial derivative notation, used previously, has been altered to a ratio of discrete differences. If it is assumed that $U_x(z_1)$, the horizontal displacement at depth, is zero, then $U_x(z_0)$ is the horizontal displacement at the surface. This same rationale was used previously to convert the shallow borehole tiltmeter observations into displacements. However, for the optical anchor, the averaging baselength is 22 m instead of 1 m.

Nearly 1 year of edited NW-SE displacement data is presented in Figure 8. A large offset occurred on day 56, 1980, at the time of a local earthquake. The 60-μm displacement recorded by the optical anchor is much larger than that deduced from the shallow borehole tiltmeters. In this case there is little doubt about the interpretation of the measurement. The surface monument for the optical anchor consists of a granite table mounted on top of a 1−m^3 concrete pad that is well cemented to the underlying material at a depth of 3.5 m. A more distant earthquake on day 288 of 1979 (Imperial Valley earthquake, $M = 6.6$, at a distance of 130 km) induced a much smaller displacement of 0.25 μm. Both of the observed static offsets were far in excess of the theoretical shear deformation expected from dislocations at the fault and must be interpreted as local adjustments of the near surface material.

For a period of 1 week prior to the local seismic event the site was subjected to heavy rainfall. Combined with the prominent offset is the response of the optical anchor to that rain. The rain induced-displacement appears to be somewhat less than the magnitude of the coincident static offset, perhaps 25 μm. This motion is present despite the optical anchor end mount being inside a 3 m by 6 m environmentally controlled vault that insulates it from direct soil moisture changes. The material on the floor of the vault is displacing nevertheless in response to the moistening of the surface layers.

With only 1 year of data it is difficult to separate the long-term trend from the cycle per year component in these measurements. After removing the step discontinuity the calculated amplitude of the annual motion is 50 μm, and the phase (for a cosine wave), relative to the start of the year, is −127° (i.e., lag). An estimate of the purely thermoelastic effect for the simple model of a tilted homogeneous elastic half space can be derived by integrating equation (1). The resulting expression is given by

$$U_x(z) = \frac{1}{4k}\,\frac{1+\sigma}{1-\sigma}\,\beta T_0 \sin(2\alpha) e^{-k(z-z_0)}\{\cos\phi + \sin\phi\}$$

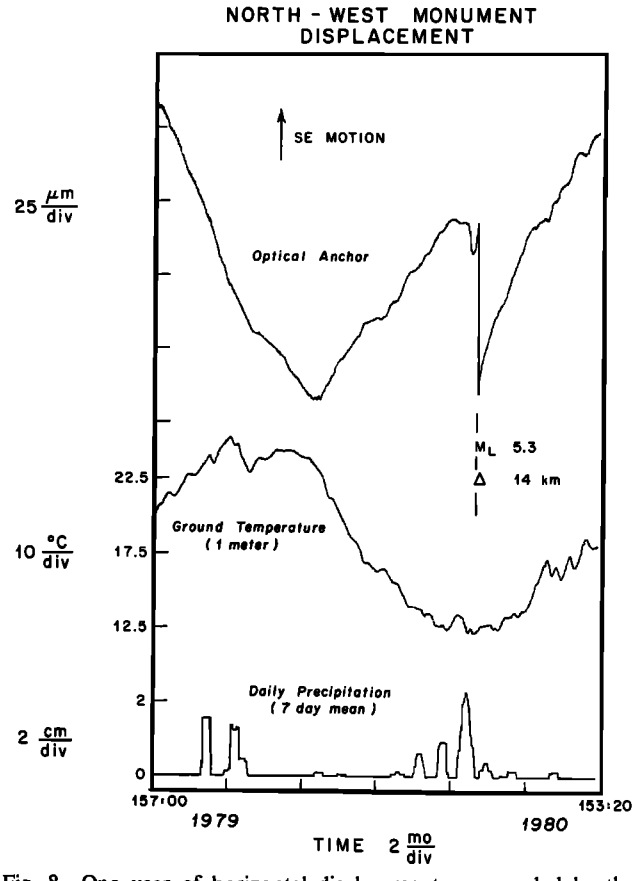

Fig. 8. One year of horizontal displacement as recorded by the optical anchor. The offset on day 56 of 1980 is due to a local earthquake. The ground temperature at a depth of 1 m and the daily precipitation are also included.

Using a depth of 3.5 m, the theoretical amplitude and phase are found to be 12.5 μm and 26°, respectively. The magnitudes are comparable; however, the phases are not in agreement. Undoubtedly, the observed signal is complicated by the strain field produced by the vault.

Thermoelastic strains are probably the source of the cycle per day component of displacement. The amplitude of the motion is 0.25 μm, much greater than can be explained by the half space model. The phase of the signal relative to 0000 UT is 29.48°, closely matching the phase of the applied surface temperature. As was noted before in the discussion of the shallow borehole tiltmeters, the amplitude of this signal tends to increase as the soil moisture decreases. These variations of the optical anchor diurnal signal are usually less than a factor of 2.

5. CONCLUSIONS

Although the observed displacements are sufficiently large to be a significant factor in crustal deformation investigations, they are less than the values generally reported for soil motion. Systematic downhill soil creep has been studied extensively (see, for example, *Carson and Kirkby* [1972]). Typically, rates of 1—2 mm/yr are observed for the top 30 cm of soil on slopes of 5° or less. Soils that are not subjected to extreme variations in temperature or moisture are found to be more stable. At PFO, below the 1-m-thick layer of soil the horizontal displacements are not predictable and are generally limited to 50 μm of motion.

A possible explanation for the displacements at Pinyon Flat is suggested by the observations of *Young* [1978]. In his 12-year study of soil creep (in northern England) he found that the principal component of particle motion was vertical rather than horizontal, as generally accepted. He attributed this to the loss of weathered material in solution with vertical settling of the remaining particles. While this hypothesis does not predict correctly the dominant motion of the soil (above 1 m) at PFO, it may explain the displacements in the heavily weathered material below the soil, where the instrumentation is emplaced. The unpredictable nature of the observed horizontal motions at a depth of 4 m may be the result of differential settling.

To this point in the description of the horizontal displacements at PFO, the discussion has been limited to the dominant features of the measurements. In fact, the various records provide us with information about the displacements that occur over a large range of frequencies. Figure 9 presents representative power spectra.

As was anticipated, the shallow borehole tiltmeter observations should be considered as a lower limit on the range of surface displacements. It is unlikely that this limit is a correct estimate of the near-surface displacements, since the baselength of the tiltmeters is very short. Assuming that the ground becomes increasingly less stable near the surface, it would be more reasonable to scale the tilt data by a length that is related to the depth of emplacement rather than the baselength of the instrument. If this were carried out, the shallow tiltmeter power levels presented in Figure 9 would be increased by 12 dB and would be more consistent with the other estimates.

The optical anchor and strainmeter end pier displacement power levels are similar, supporting the models presented in the previous section. The expected standard deviation of the horizontal displacements in a specified frequency interval may be estimated using the levels presented in Figure 9. First the power spectral density is integrated over the desired range of frequencies. Then the square root of this quantity is calculated, providing an estimate of the standard deviation. For the power spectra presented, the largest signals are expected at the lowest frequencies. The standard deviation of displacements in the period range 2—19 months is approximately 50 μm.

The magnitude of this displacement serves as a constraint in the design of geophysical instrumentation. There is considerable evidence establishing that the rate of normal crustal deformations in a tectonically active region, such as California, is of the order of 0.1 $\mu\epsilon$/yr [*Savage et al.*, 1981]. In order to determine the characteristics of these signals an instrument must be capable of accurately monitoring variations that are a fraction of this level. This may be accomplished in different ways. One solution is to extend the baselength of the instrumentation to a length such that the expected monument displacements are a small fraction of the signal levels [e.g., *Huggett et al.*, 1977]. Or, on the basis of the assumption that the crustal materials become more stable with depth, an instrument such as the optical anchor may be employed to monitor monument displacements. Finally, it is possible that locating observing sites on material more stable than that at PFO would reduce the monument noise.

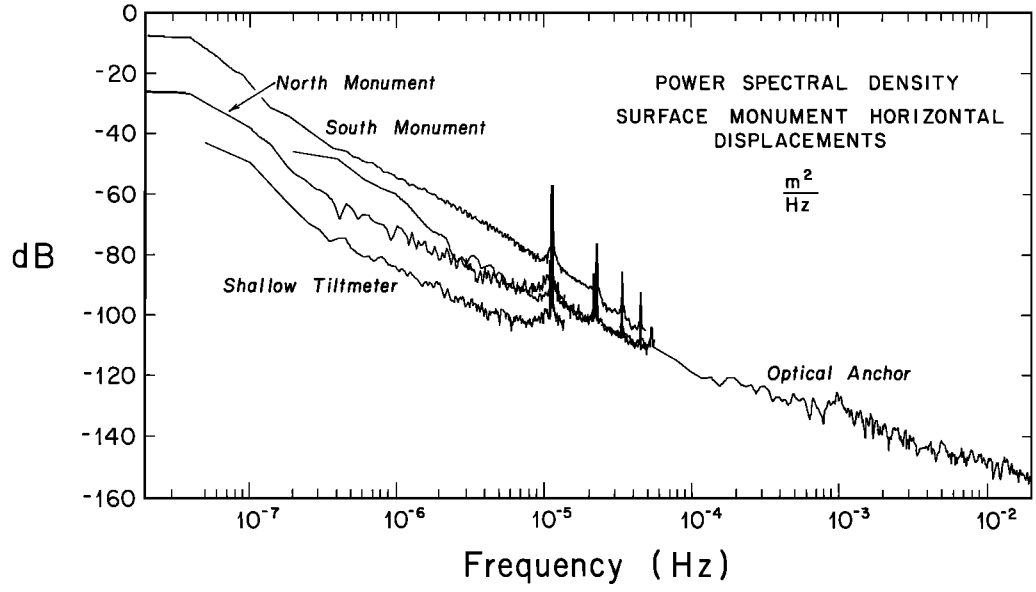

Fig. 9. Power spectral density of the near-surface horizontal displacements in weathered granodiorite. Included are the power levels recorded by the optical anchor and those inferred from the monument tiltmeter and the shallow borehole tiltmeter records.

Certainly, the last approach is the best solution. However, it may not be easily accomplished. The character of the near-surface material at PFO, as well as the smoothly varying terrain at the site, are well suited for geophysical instrumentation. To date there is no evidence that areas of rock outcrops or tunnel floors provide a more stable platform for horizontal strain measurements. Further, both areas have features that restrict the use of a variety of equipment.

Extending the baselength of the instrumentation is also difficult. Assuming that the monument displacements are independent, the differential motion of two monuments should be $2^{1/2}$ times the value determined above (50 μm). In order to reduce the standard deviation of the error in measuring horizontal deformation to the level of 0.01 $\mu\epsilon$/yr, a baselength of 7 km would be needed. It is not practical to build a controlled environment (such as an evacuated optical path) over these distances. Experimental programs to improve the accuracy of measurements through the atmosphere will thus be necessary.

Until such techniques have been developed, sophisticated reference monuments will be required if observatory-based experiments are to record tectonic deformations faithfully.

Acknowledgments. I wish to thank Duncan Carr Agnew for his thorough review of this paper and Jon Berger for his support in conducting the many lengthy experiments. Many of the ideas presented here are the results of discussion with these individuals. This work was supported by the National Science Foundation, the United States Geological Survey, and the National Aeronautics and Space Administration.

REFERENCES

Agnew, D. C., Strain tides at Piñon Flat: Analysis and interpretation, Ph.D. thesis, Inst. of Geophys. and Planet. Phys., Univ. of Calif., San Diego, 1979.

Agnew, D. C., Nonlinearity in rock: Evidence from earth tides, *J. Geophys. Res., 86*, 3969–3878, 1981.

Berger, J., and J. Levine, The spectrum of earth strain from 10^{-8} to 10^{2} Hz, *J. Geophys. Res., 79*, 1210–1214, 1974.

Berger, J., and R. H. Lovberg, Earth strain measurements with a laser interferometer, *Science, 170*, 296–303, 1970.

Birch, F., The velocity of compressional waves in rocks to 10 kilobars, Part 1., *J. Geophys. Res., 65*, 1083–1102, 1960.

Carson, M. A., and M. J. Kirkby, *Hillslope Form and Process*, Cambridge University Press, New York, 1972.

Cooke, R. U., and A. Warren, *Geomorphology in Deserts*, University of California Press, Berkeley, 1973.

Foster, J., Geology, in *Deep Canyon, a Desert Wilderness for Science*, edited by I. P. Ting and W. Jennings, pp. 90–91, University of California, Riverside, 1976.

Garmany, J., J. A. Orcutt, and R. L. Parker, Travel time inversion: A geometric approach, *J. Geophys. Res. 84*, 3615–3622, 1979.

Harrison, J. C., and K. Herbst, Thermoelastic strains and tilts revisited, *Geophys. Res. Lett., 4*, 535–537, 1977.

Huggett, G. R., L. E. Slater, and J. Langbein, Fault slip episodes near Hollister, California: Initial results using a multiwavelength distance-measuring instrument, *J. Geophys. Res., 82*, 3361–3368, 1977.

Isherwood, D., and A. Street, Biotite-induced grussification of the Boulder Creek granodiorite, Boulder County, Colorado, *Geol. Soc. Am. Bull., 87*, 366–370, 1976.

Jahns, R. H., Geology of the Peninsular Range Province, southern California and Baja California, in *Geology of Southern California, Bull. 170*, edited by R. H. Jahns, pp. 29–52, California Division of Mines, San Francisco, 1954.

Johnston, M. J. S., Testing the physical parameters of short baseline tiltmeters intended for earthquake prediction, *U.S. Geol. Surv. Open File Rep., 76-556*, 1976.

Morrissey, S.-T., Special technical report: A study on the adaptation of a commercial tiltmeter for monitoring earth tilts in unfavorable environments, technical report contract USDIGS 14-08-0001-15048, U.S. Geol. Surv., Menlo Park, Calif., April 29, 1977.

Rogers, T. H., Santa Ana sheet, in *Geologic Map of California*, edited by O. P. Jenkins, Division of Mines and Geology, Sacramento, California, 1965.

Savage, J. C., W. H. Prescott, M. Lisowski, and N. E. King, Strain accumulation in southern California, 1973–1980, *J. Geophys. Res., 86*, 6991–7001, 1981.

Sharp, R. V., San Jacinto fault zone in the Peninsular Ranges of southern California, *Geol. Soc. Am. Bull., 78*, 705–730, 1967.

Thatcher, W., J. A. Hileman, and T. C. Hanks, Seismic slip distribution along the San Jacinto fault zone, southern California,

and its implications, *Geol. Soc. Am. Bull., 86*, 1140–1146, 1975.
Wahrhaftig, C., Stepped topography of the southern Sierra Nevada, California, *Geol. Soc. Am. Bull., 76*, 1165–1190, 1965.
Wood, M. D., and N. E. King, Relation between earthquakes, weather, and soil tilt, *Science, 197*, 154–156, 1977.
Wyatt, F., Theoretical and observed surface deformations due to a distant earthquake (abstract), *Eos Trans. AGU, 61*, 211, 1980.
Wyatt, F., and J. Berger, Investigations of tilt measurements using shallow borehole tiltmeters, *J. Geophys. Res., 85*, 4351–4362, 1980.
Wyatt, F., K. Beckstrom, and J. Berger, The optical anchor—A geophysical strainmeter, submitted to *Bull. Seismol. Soc. Am.*, 1982.
Young, A., A twelve-year record of soil movement on a slope, *Z. Geomorphol. Suppl. 29*, 104–110, 1978.

(Received May 6, 1981;
revised September 8, 1981;
accepted September 18, 1981.)